

Frequency conversion over two-thirds of an octave in silicon nanowaveguides

Amy C. Turner-Foster¹, Mark A. Foster², Reza Salem², Alexander L. Gaeta², and Michal Lipson^{1*}

¹*School of Electrical and Computer Engineering, Cornell University, Ithaca, NY 14853, U.S.A.*

²*School of Applied and Engineering Physics, Cornell University, Ithaca, NY 14853, U.S.A.*

*lipson@ece.cornell.edu

Abstract: We demonstrate ultrabroad-bandwidth low-power frequency conversion of continuous-wave light in a dispersion engineered silicon nanowaveguide via four-wave mixing. Our process produces continuously tunable four-wave mixing wavelength conversion over two-thirds of an octave from 1241-nm to 2078-nm wavelength light with a pump wavelength in the telecommunications C-band.

©2010 Optical Society of America

OCIS codes: (130.7405) Wavelength conversion devices; (190.4390) Integrated optics.

References and links

1. H. Rong, Y.-H. Kuo, A. Liu, M. Paniccia, and O. Cohen, "High efficiency wavelength conversion of 10 Gb/s data in silicon waveguides," *Opt. Express* **14**(3), 1182–1188 (2006), <http://www.opticsinfobase.org/abstract.cfm?URI=oe-14-3-1182>.
2. Y.-H. Kuo, H. Rong, V. Sih, S. Xu, M. Paniccia, and O. Cohen, "Demonstration of wavelength conversion at 40 Gb/s data rate in silicon waveguides," *Opt. Express* **14**(24), 11721–11726 (2006), <http://www.opticsinfobase.org/oe/abstract.cfm?URI=oe-14-24-11721>.
3. V. Ta'eed, M. D. Pelusi, B. J. Eggleton, D.-Y. Choi, S. Madden, D. Bulla, and B. Luther-Davies, "Broadband wavelength conversion at 40 Gb/s using long serpentine As₂S₃ planar waveguides," *Opt. Express* **15**(23), 15047–15052 (2007), <http://www.opticsinfobase.org/oe/abstract.cfm?URI=oe-15-23-15047>.
4. B. G. Lee, A. Biberman, A. C. Turner-Foster, M. A. Foster, M. Lipson, A. L. Gaeta, and K. Bergman, "Demonstration of broadband wavelength conversion at 40 Gb/s in silicon waveguides," *IEEE Photon. Technol. Lett.* **21**(3), 182–184 (2009).
5. Th. Udem, R. Holzwarth, and T. W. Hänsch, "Optical frequency metrology," *Nature* **416**(6877), 233–237 (2002).
6. M. A. Foster, R. Salem, D. F. Geraghty, A. C. Turner-Foster, M. Lipson, and A. L. Gaeta, "Silicon-chip-based ultrafast optical oscilloscope," *Nature* **456**(7218), 81–84 (2008).
7. M. A. Foster, R. Salem, Y. Okawachi, A. C. Turner-Foster, M. Lipson, and A. L. Gaeta, "Ultrafast waveform compression using a time-domain telescope," *Nat. Photonics* **3**(10), 581–585 (2009).
8. H. Rong, S. Xu, O. Cohen, O. Raday, M. Lee, V. Sih, and M. Paniccia, "A cascaded silicon Raman laser," *Nat. Photonics* **2**(3), 170–174 (2008).
9. D. Dimitropoulos, V. Raghunathan, R. Claps, and B. Jalali, "Phase-matching and nonlinear optical processes in silicon waveguides," *Opt. Express* **12**(1), 149–160 (2004), <http://www.opticsinfobase.org/abstract.cfm?URI=oe-12-1-149>.
10. V. Raghunathan, R. Claps, D. Dimitropoulos, and B. Jalali, "Parametric Raman wavelength conversion in scaled silicon waveguides," *J. Lightwave Technol.* **23**(6), 2094–2102 (2005).
11. R. L. Espinola, J. I. Dadap, R. M. Osgood, Jr., S. J. McNab, and Y. A. Vlasov, "C-band wavelength conversion in silicon photonic wire waveguides," *Opt. Express* **13**(11), 4341–4349 (2005), <http://www.opticsinfobase.org/abstract.cfm?URI=oe-13-11-4341>.
12. H. Fukuda, K. Yamada, T. Shoji, M. Takahashi, T. Tsuchizawa, T. Watanabe, J. Takahashi, and S. Itabashi, "Four-wave mixing in silicon wire waveguides," *Opt. Express* **13**(12), 4629–4637 (2005), <http://www.opticsinfobase.org/abstract.cfm?URI=oe-13-12-4629>.
13. M. A. Foster, A. C. Turner, J. E. Sharping, B. S. Schmidt, M. Lipson, and A. L. Gaeta, "Broad-band optical parametric gain on a silicon photonic chip," *Nature* **441**(7096), 960–963 (2006).
14. K. Yamada, H. Fukuda, T. Tsuchizawa, T. Watanabe, T. Shoji, and S. Itabashi, "All-optical efficient wavelength conversion using silicon photonic wire waveguide," *IEEE Photon. Technol. Lett.* **18**(9), 1046–1048 (2006).
15. Q. Lin, J. Zhang, P. M. Fauchet, and G. P. Agrawal, "Ultrabroadband parametric generation and wavelength conversion in silicon waveguides," *Opt. Express* **14**(11), 4786–4799 (2006), <http://www.opticsinfobase.org/abstract.cfm?URI=oe-14-11-4786>.
16. M. A. Foster, A. C. Turner, R. Salem, M. Lipson, and A. L. Gaeta, "Broad-band continuous-wave parametric wavelength conversion in silicon nanowaveguides," *Opt. Express* **15**(20), 12949–12958 (2007), <http://www.opticsinfobase.org/oe/abstract.cfm?URI=oe-15-20-12949>.

17. R. Salem, M. A. Foster, A. C. Turner, D. F. Geraghty, M. Lipson, and A. L. Gaeta, "Signal regeneration using low-power four-wave mixing on silicon chip," *Nat. Photonics* **2**(1), 35–38 (2008).
18. A. C. Turner, M. A. Foster, A. L. Gaeta, and M. Lipson, "Ultra-low power parametric frequency conversion in a silicon microring resonator," *Opt. Express* **16**(7), 4881–4887 (2008), <http://www.opticsinfobase.org/oe/abstract.cfm?URI=oe-16-7-4881>.
19. E. Dulkeith, F. Xia, L. Schares, W. M. J. Green, and Y. A. Vlasov, "Group index and group velocity dispersion in silicon-on-insulator photonic wires," *Opt. Express* **14**(9), 3853–3863 (2006), <http://www.opticsinfobase.org/abstract.cfm?URI=oe-14-9-3853>.
20. A. C. Turner, C. Manolatu, B. S. Schmidt, M. Lipson, M. A. Foster, J. E. Sharping, and A. L. Gaeta, "Tailored anomalous group-velocity dispersion in silicon channel waveguides," *Opt. Express* **14**(10), 4357–4362 (2006), <http://www.opticsinfobase.org/oe/abstract.cfm?URI=oe-14-10-4357>.
21. M. E. Marhic, N. Kagi, T. K. Chiang, and L. G. Kazovsky, "Broadband fiber optical parametric amplifiers," *Opt. Lett.* **21**(8), 573–575 (1996), <http://www.opticsinfobase.org/ol/abstract.cfm?URI=ol-21-8-573>.
22. R. Jones, H. Rong, A. Liu, A. Fang, M. Paniccia, D. Hak, and O. Cohen, "Net continuous wave optical gain in a low loss silicon-on-insulator waveguide by stimulated Raman scattering," *Opt. Express* **13**(2), 519–525 (2005), <http://www.opticsinfobase.org/abstract.cfm?URI=oe-13-2-519>.
23. H. Rong, R. Jones, A. Liu, O. Cohen, D. Hak, A. Fang, and M. Paniccia, "A continuous-wave Raman silicon laser," *Nature* **433**(7027), 725–728 (2005).
24. A. C. Turner-Foster, M. A. Foster, J. S. Levy, C. B. Poitras, R. Salem, A. L. Gaeta, and M. Lipson, "Ultrashort free-carrier lifetime in low-loss silicon nanowaveguides," submitted for publication (2009).
25. V. R. Almeida, R. R. Panepucci, and M. Lipson, "Nanotaper for compact mode conversion," *Opt. Lett.* **28**(15), 1302–1304 (2003), <http://www.opticsinfobase.org/ol/abstract.cfm?URI=ol-28-15-1302>.

1. Introduction

The ability to generate and utilize large bandwidths using parametric processes is crucial for a large range of photonic applications including signal processing and communications [1–4], optical frequency metrology [5], ultrafast all-optical processing [6,7], and spectroscopy [8]. The past several years have seen much research focused on the nonlinear optical process of four-wave mixing (FWM) in silicon waveguides for low-power wavelength conversion in a compact device [1,2,4,9–18]. More recently the design of these structures has focused on extending the bandwidth of the process through careful control of the group-velocity dispersion [13,15,16,19,20] since in the low-gain limit, the bandwidth of the degenerate pump FWM process is inversely proportional to the square root of the product of the interaction length and the group-velocity dispersion (GVD) parameter [16,21]. The large effective nonlinearity of silicon nanowaveguides enables efficient nonlinear processes in short cm-long waveguides, which combined with the ability to tailor the GVD [19,20], allows the process of FWM to be optimized for very large conversion bandwidths [13,15,16]. Nevertheless, maximal FWM conversion bandwidths have not yet been observed due to difficulties in placing the zero-GVD (ZGVD) point within the tuning range of a high-power pump laser.

Here, we investigate continuous-wave (CW) FWM in silicon waveguides with the first ZGVD point near the center of the C-band where high-power pump lasers are readily available. We observe an extremely broad conversion bandwidth of 837 nm which allows for continuously tunable wavelength conversion from 1241 nm to 2078 nm with a pump wavelength of 1554 nm.

2. Device design and fabrication

The silicon rib waveguide must be carefully designed to place its first ZGVD point near the center of the telecommunications C-band. Previously we experimentally demonstrated conversion bandwidths of approximately 160 nm but were limited to operating in proximity to the second ZGVD point where strong effects from fourth-order dispersion (FOD) were observed [16]. Here, we have designed and fabricated a waveguide whose first ZGVD point is within the C-band, which provides a reduction in the FOD at the pump wavelength by more than two orders of magnitude from 5×10^{-4} ps⁴/m to 1×10^{-6} ps⁴/m. This reduction in the FOD along with the ability to operate very near the ZGVD point enable the ultrabroad-bandwidth conversion observed here.

The rib design of our silicon waveguide allows for compatibility with electrical control of carrier removal for future devices [22–24]. The waveguide consists of a silicon channel waveguide on top of a thin silicon slab (inset, Fig. 1). The height of the silicon waveguide at

its thickest point is designed to be 300 nm, and the slab thickness is 30 nm. We simulate the effective index as a function of wavelength using a custom finite-difference mode solver including material dispersion of the silicon, buried thermal silicon dioxide and plasma-enhanced chemical vapor deposited silicon dioxide (PECVD-oxide) cladding and we numerically differentiate the dependence to determine the GVD as a function of wavelength for a range of waveguide widths [20]. From our simulations, we determine the ideal waveguide width to be 700 nm for a first ZGVD point very close to 1550 nm. Figure 1 shows the simulated GVD for the TE-like mode for this waveguide width and waveguides widths within ± 20 nm. From these simulations, it is clear that changing the width of the waveguide by only 10 nm can shift the ZGVD point by more than 12 nm. Furthermore, we have found that a 10-nm change in etch depth leads to approximately a 27-nm shift in the ZGVD wavelength. Since the telecommunications C-band is approximately 30-nm wide (from 1535 nm to 1565 nm), this sensitivity leads to strict dimensional tolerances in the fabrication. Utilizing state-of-the-art nanofabrication techniques such as electron beam lithography with nanometer resolution allows us to comfortably define the width of our devices within the specified tolerances and the proper etch depth is realized through precise calibration of the etch rate in the inductively coupled plasma reactive ion etcher.

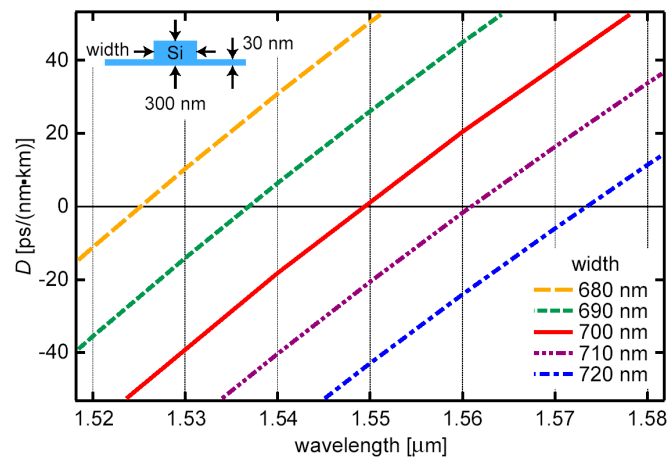


Fig. 1. Simulated group-velocity dispersion (GVD) for waveguides with a slab of 30 nm, a height of 300 nm and five different waveguide widths varied in 10-nm increments for the TE-like mode. As the width is varied by 10 nm, the ZGVD wavelength shifts by approximately 12 nm. Inset: Schematic of waveguide cross-section.

The first simulated ZGVD point for the ideally-designed waveguide is located at a wavelength of 1549 nm. The designed device is fabricated in the silicon layer of a silicon-on-insulator wafer with a buried oxide of 3 μm . The waveguides are patterned in hydrogen silsesquioxane with an electron-beam lithography tool and etched to an etch depth of 270 nm in a Cl/BCl_3 environment using an inductively coupled plasma reactive ion etcher. The waveguides are then clad with 3 μm of silicon dioxide from a plasma-enhanced chemical vapor deposition (PECVD) tool. The finished devices are diced and polished to the end of the nanotaper mode converter [25] for optical testing.

3. Experiment

We use a tunable CW C-band laser as the pump, and several tunable CW lasers spanning the O- E- S- and C-bands (1250 nm - 1565 nm) are employed for the signal. The laser light from the pump laser is sent through an EDFA, and the signal and pump are individually sent through polarization controllers and then combined with a commercially available fiber-based wavelength-division multiplexer (WDM). The combined signal and pump are coupled into our silicon waveguide using a lensed fiber and inverse nanotapers for mode conversion [25]. The FWM process occurs in the 1.5-cm-long silicon waveguide, and the output is coupled

through an inverse nanotaper and collected into a fiber and sent to a long-wavelength optical spectrum analyzer (OSA) sensitive to wavelengths from 1200 nm to 2200 nm.

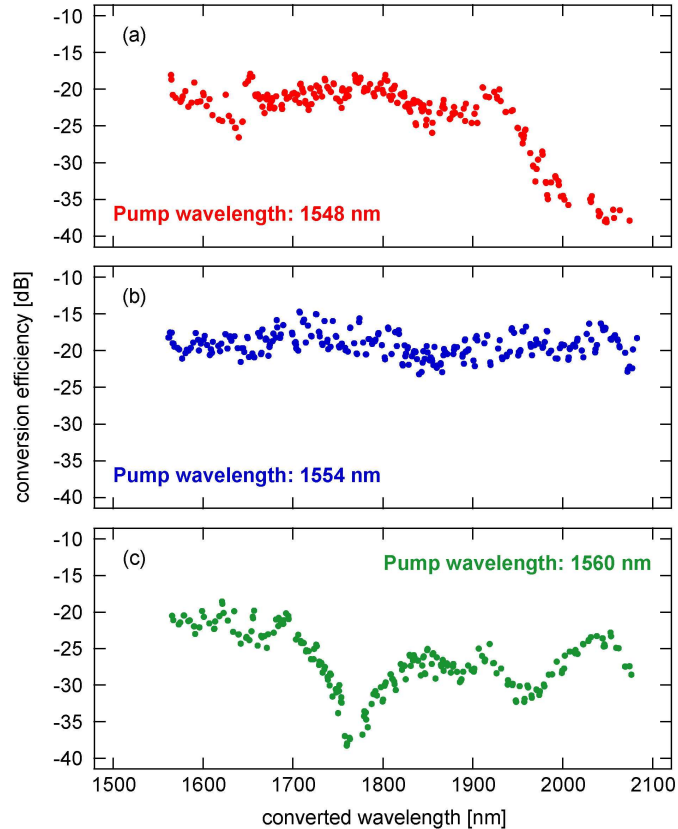


Fig. 2. Experimentally measured on-off conversion efficiency with 110 mW input pump power as a function of converted wavelength for pump wavelength of (a) 1548 nm, (b) 1554 nm, and (c) 1560 nm. Pumping at 1554 nm yields the largest conversion bandwidth of > 837 nm. For this pump wavelength the measured conversion bandwidth is limited only by the tuning range of our signal laser.

The pump and signal are launched into the TE-like mode of the waveguide through the inverse nanotaper. The average power of the pump and signal in the waveguide are 110 mW and 250 μ W, respectively. The conversion bandwidth is highly dependent on the location of the pump wavelength with respect to the ZGVD point of the waveguide. We position the CW pump near the predicted ZGVD point and continuously tune our CW signal between 1241 nm and the pump wavelength. The pump wavelength is then adjusted to maximize the conversion bandwidth. In Fig. 2, we plot the on-off conversion efficiency as a function of converted wavelength for three different pump wavelengths. As shown in Fig. 2(b), we find a maximum conversion bandwidth for a pump wavelength of 1554 nm. In fact, for this pump wavelength the measured conversion bandwidth is only limited by the tuning range of our signal. As the signal is tuned from 1241 nm to the pump wavelength the FWM interaction generates narrowband CW light at wavelengths ranging from 2078 nm to the pump wavelength as determined by energy conservation. A sample trace of the conversion from 1250 nm to 2056 nm with the pump centered at 1554.7 nm is shown in Fig. 3. We detect the power in the converted wave using the OSA and compare this power to the signal power exiting the waveguide in the absence of the pump to determine the on-off conversion efficiency [9–14,16–18]. As we increase the pump power, we find that the on-off conversion efficiency saturates near -18 dB. Although we are operating with 110 mW of pump power, we see the

efficiency begins to saturate at 30 mW. The conversion efficiency is reduced compared to previous demonstrations due to the longer free-carrier lifetime in these waveguides (3 ns here as compared to 500 ps in Ref. 16), which results from the larger cross-section required to place the first ZGVD point in the C-band. However, this conversion efficiency can be significantly improved through the integration of a *p-i-n* diode to rapidly remove the generated free-carriers [1,2,22–24].

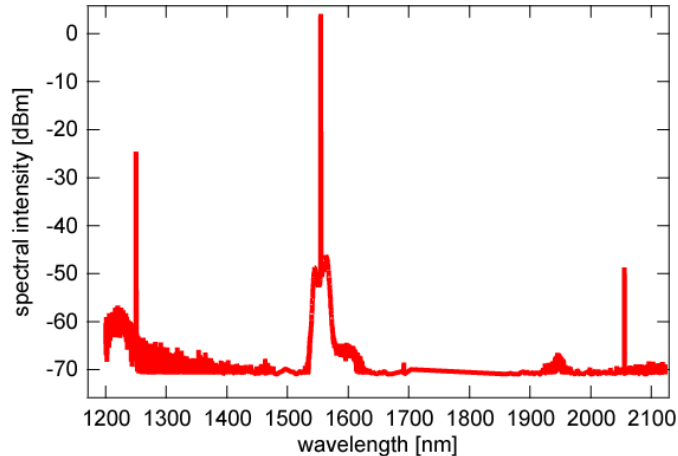


Fig. 3. Sample FWM trace of signal light converted from a wavelength of 1250 nm to 2056 nm with a pump wavelength of 1554.7 nm.

By tuning the pump wavelength away from the ZGVD point the conversion bandwidth decreases. For a short pump wavelength of 1548 nm, we experimentally observe the conversion bandwidth extending to 1930 nm and then decreasing significantly as shown in Fig. 2(a). For a long pump wavelength of 1560 nm, the primary experimental conversion bandwidth extends only to 1760 nm with very sharp oscillatory features thereafter as shown in Fig. 2(c). Using the observed conversion bandwidths for the pump at 1548 nm and 1560 nm we can estimate the GVD parameter at these wavelengths. From these measurements we calculate a dispersion slope of 1.6 ps/nm²·km, which agrees closely with the simulated dispersion slope of 1.9 ps/nm²·km.

4. Conclusion

We demonstrate low-power four-wave mixing wavelength conversion that is continuously tunable over two-thirds of an octave using silicon nanowaveguides. This device allows the generation of narrow-linewidth CW light continuously tunable from the telecommunications C-band to 2078 nm using standard commercially-available telecommunications equipment. The ability to parametrically convert light over this ultra-broad-bandwidth gives rise to new functionality for silicon photonics and can have application in spectroscopy, ultrafast optical processing and measurement, and optical frequency metrology.

Acknowledgements

This work was funded by the DARPA MTO POPS Program and the Cornell Center for Nanoscale Systems, supported by the NSF and the New York State Office of Science, Technology and Academic Research. M.A.F., R. S., and A.L.G. also acknowledge support under the DARPA DSO Slow-Light Program. This work was performed in part at the Cornell NanoScale Science and Technology Facility, a member of the National Nanotechnology Infrastructure Network, which is supported by the National Science Foundation.